J. Eur. Opt. Society-Rapid Publ. 2024, **20**, 37
© The Author(s), published by EDP Sciences, 2024
https://doi.org/10.1051/jeos/2024039
Available online at: https://jeos.edpsciences.org

Journal of the European Optical Society-Rapid Publications

SHORT COMMUNICATION OPEN ACCESS

Design of composite optical nanofibers for new all-solid-state Raman wavelength converters

Sylvie Lebrun[1,*], Maha Bouhadida[1], Théo Dampt[2], Mathieu Fauvel[2], Christian Larat[2], Abderrahim Azzoune[1,3], Jean-Charles Beugnot[4], and Laurent Divay[2]

[1] Université Paris-Saclay, Institut d'Optique Graduate School, CNRS, Laboratoire Charles Fabry, 91127 Palaiseau, France
[2] Thales Research and Technology, 91767 Palaiseau Cedex, France
[3] Ecole Militaire Polytechnique, Laboratoire Systèmes Lasers, BP17, 16111 Bordj-El-Bahri, Algiers, Algeria
[4] Institut Femto-ST, CNRS, Université Bourgogne, Franche-Comté, 25030 Besançon, France

Received 25 July 2024 / Accepted 2 October 2024

Abstract. We present the design of composite optical nanofibers (ONF) coated with thin layers of nonlinear materials, Titanium dioxyde (TiO_2) and Polymethyl methacrylate (PMMA), for the realization of new all-solid Raman wavelength converters for an emission around 1.5 µm. Our simulations show that Stimulated Raman Scattering can be obtained with moderate input peak powers, typical ONF geometrical parameters, and layer thicknesses deposited which are technologically achievable: a few tens of nm for TiO_2 and a few hundreds of nm for PMMA. This study enlarges the field of applications of ONF in nonlinear optics and lasers by opening the way to the coating by other materials such as doped polymers.

Keywords: Silica nanofiber, Raman converter, Nonlinear optics, TiO_2, PMMA.

1 Introduction and motivations

Optical nanofiber (ONF), i.e., the homogeneous section of a stretched and tapered silica optical fiber (sub-micrometer or micrometer diameter on length of up to more than 10 cm) between two tapered transitions, has been widely used in science and engineering applications since more than thirty years as an elementary optical component easily integrated by its nature in an all-fibered network [1]. Due to these intrinsic properties, ONF-based technologies have addressed a large versatility of domains from fundamental to applications such as quantum information devices (e.g. trapped atoms for quantum light-matter interfaces, photon-pair generation) [2, 3], remote sensor devices [4], nonlinear optics (e.g. supercontinuum generation) [5] for the most active ones. The expanding use of ONF is due to its physical properties. The optical modes guided by the ONF have large intensities due to their strong transverse confinement, present very low losses (below 0.005 dB/cm, far beyond other micro/nano waveguides), and exhibit an evanescent part outside the ONF and therefore in interaction with the external medium. In nonlinear optics, only a few experimental demonstrations using the evanescent field in ONF have been reported [6, 7]. In these studies, the ONF serves as the optical waveguide, and the nonlinear medium is constituted by the immersing liquid. Among them, we report highly efficient wavelength converters based on Stimulated Raman Scattering (SRS) in the evanescent field of ONF immersed in liquids. The pump photons in the evanescent field scatter by SRS on the molecules of the liquid. Then the generated Stokes photons couple to a propagating mode of the ONF and are collected at the output of the end fiber. Conversion efficiencies from the pump source emitting at 532 nm to the first Stokes order of ethanol at 630 nm as high as 60% were obtained in the sub-nanosecond regime [6]. For a given pump wavelength, changing the immersing liquid enables to change of the Stokes wavelength, opening the way to a new family of liquid Raman converters. Due to the absorption of liquids in the near-infrared range, these converters are optimized for visible wavelengths. Despite these attractive features, the performances were limited by the optical breakdown of the ONF induced by the pump laser [8]. The absorption of the laser by surface defects can lead to an increase of the temperature of the ONF and in its vicinity generating bubbles in the liquid that can degrade the optical transmission and even break the ONF.

In this work, we investigate new possibilities offered by silica ONF coated with thin films of nonlinear materials. The aim is to build all-solid Raman wavelength converters in the pulsed regime based on these so-called "composite ONF". The light propagation is ensured by the ONF and

* Corresponding author: sylvie.lebrun@institutoptique.fr

the nonlinear photons produced in the coating layer coupled to a propagating mode of the composite ONF. This mode is then collected at the output end fiber. The selected materials for the coatings are Titanium dioxyde (TiO_2) and Polymethyl methacrylate (PMMA). These materials are both transparent in the visible, near visible range, and in the telecommunication window. TiO_2 is a highly nonlinear material and has been used for the realization of integrated waveguides under its crystalline phase [9]. PMMA is also an interesting material for nonlinear optics [10]. As an example, PMMA optical fibers have been studied for Raman amplifiers. This material is also known for its relatively high laser-damage resistance. For both materials, an original process for the coating of ONF with thin layers of controlled thicknesses has been developed. The present article is theoretical but the data used for the simulations are based on realistic ones obtained from experiments described in [11]. Due to their small diameter, the evanescent field of the propagating mode in ONF is very sensitive to dust and pollutants that can be deposited on its surface. These are known to be responsible for degradation of the optical transmission of ONF. The refractive indexes of the chosen nonlinear materials being higher than the one of silica, we will see that the thicknesses of TiO_2 and PMMA layers should be respectively a few tens of nm and a few hundreds of nm to keep the guidance on the fundamental modes. Such thicknesses are also achievable technically. However, they are not sufficient to fully protect the evanescent field that typically spreads on a few μm. That is why we also studied theoretically in the present work and experimentally in [11] the encapsulation of a PMMA-coated ONF with a low-index material, silicone, for additional protection. In this work, the targeted Stokes wavelengths are in the telecommunication window but they can be extended to other wavelength ranges where the materials are transparent.

This article is organized as follows:

After a description of the all-solid wavelength converters, we introduce the calculation of the Raman modal gain which is the key parameter to design the geometry of the ONF (length and radius) and the thickness of the coating. Then we present the results of the simulations for the two studied configurations, an ONF coated with TiO_2 (ONF 1) and an ONF coated with PMMA (ONF 2). In this last case, the ONF with the layer of PMMA is encapsulated in a low-index polymer of silicone for additional mechanical protection. Based on our previous results obtained in liquids, we show the conditions under which SRS can be obtained in these composite ONFs. Above these preliminary results, this study opens the way to a new family of all-fibered components with functionalizations that can be tailored thanks to the coating of an ONF with different nonlinear materials.

2 General design of all-solid Raman converters based on a composite ONF

The composite ONF is a three-layer step-index waveguide, constituted by silica, the nonlinear material, and the surrounding material that can be air or an encapsulation material. In the simulations we have performed, the thickness of the material used for encapsulation is considered infinite. The length of the silica ONF is L and its radius is r_{NF}. The thickness of the nonlinear material deposited on the ONF is e. We consider propagation on the fundamental mode at both pump and Stokes wavelengths. To calculate the field profiles, we have used the classical three-layer model in the scalar approximation described in [12]. Following this method, we first calculate the effective indexes of the modes at both wavelengths by solving eigenvalue equations obtained by writing the continuity conditions on the fields at the interfaces and then derive the electric and magnetic fields in each layer of the waveguide. As the refractive indexes of the nonlinear materials are in general higher than the one of silica, the thickness of the deposited layers should enable the guidance on the fundamental modes at both wavelengths. In particular, it means that for each ONF diameter we have to find a range of thicknesses in which the effective index lie between the refractive index of the external medium (air or silicone) and the refractive index of the nonlinear medium.

The key parameter for the design of our component is the Raman modal gain g_{Rmod} (in $\mathrm{m^{-1}\ W^{-1}}$). The modal Raman gain is expressed following the analysis conducted in [13] by:

$$g_{\mathrm{Rmod}} = \frac{\varepsilon_0^2 c^2 \int_{\text{active area}} g_{\mathrm{bulk}} n_g^2 |e_p \cdot e_s|^2 \mathrm{d}A}{\left(\int_{\text{total area}} (e_p \times h_p) \cdot z \mathrm{d}A\right)\left(\int_{\text{total area}} (e_s \times h_s) \cdot z \mathrm{d}A\right)},$$

ε_0 is the dielectric permittivity of vacuum, c is the celerity of light in vacuum, $\mathrm{d}A$ is a unitary surface element and z is the direction of propagation. This gain is depending on the parameters of the nonlinear material which are its Raman gain coefficient g_{bulk} (in $\mathrm{mW^{-1}}$) and its refractive index n_g; e and h represent, respectively, the electric and the magnetic fields; p and s stand for, respectively, pump and Stokes. We consider that the pump and the Stokes modes are both scalar and propagate on the fundamental mode which presents a revolution symmetry.

To size our component, we are based on our previous results obtained in liquids in the sub-nanosecond regime. We were able to observe SRS with ONF lengths of 4–8 cm, peak pump powers of a few hundreds of W, and moderate modal Raman gains that can be down to 0.2 $\mathrm{m^{-1}\ W^{-1}}$ [6]. Moreover, in [6], we showed that the experimental data were in good agreement with the theory at the Raman threshold, confirming that the calculation of the modal Raman gain as exposed above is accurate.

For the simulations, we decide to target a modal Raman gain of 0.2 $\mathrm{m^{-1}\ W^{-1}}$. A lower modal Raman gain can be compensated by a longer ONF or an increase of the input pump power.

3 ONF coated with TiO_2 (ONF 1)

For this study, the pump wavelength is 1.5 μm. As the Raman shift of TiO_2 is small (140 $\mathrm{cm^{-1}}$), the first Stokes

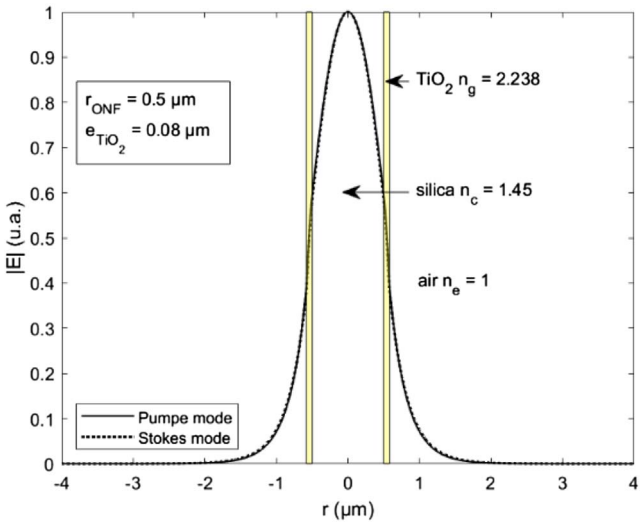

Figure 1. Profile of the pump and Stokes modes propagating in an ONF having a radius of 500 nm, coated by an 80 nm thick layer of TiO_2.

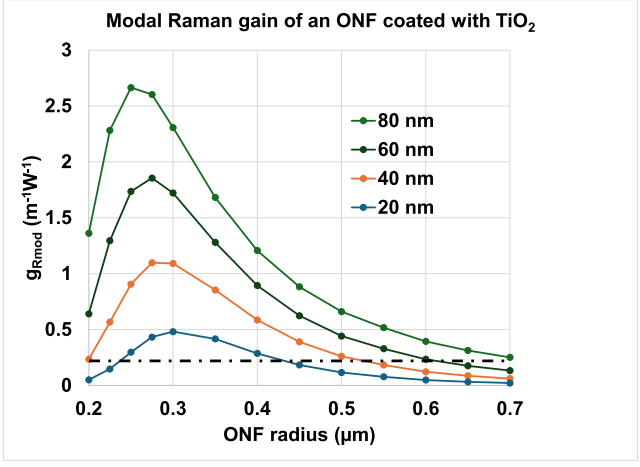

Figure 2. Modal Raman gain versus the ONF radius in function of the thickness of the TiO_2 layer.

order wavelength is close, at 1.54 µm. The deposition of thin layers of TiO_2 is performed by Atomic Layer Deposition, leading to deposited layers of a few tens of nm thick. With this technique, the deposited TiO_2 is amorphous which implies that its refractive index is lower than for its crystalline phases. We measured a refractive index of 2.239 at 1.5 µm. The Raman gain coefficient of TiO_2 is 6.6 10^{-12} mW^{-1} [9].

Figure 1 shows an example of calculated spatial modes at the pump and Stokes wavelengths for a silica ONF radius of 0.5 µm and an 80 nm thick TiO_2 layer. These fundamental mode profiles do not change globally with the ONF radius, keeping a Gaussian-like shape. One can notice the very strong overlap between pump and Stokes modes, due to the small wavelength difference between these two waves.

In Figure 2 we have plotted the modal Raman gain of ONF 1 *versus* the silica ONF radius for deposited layers

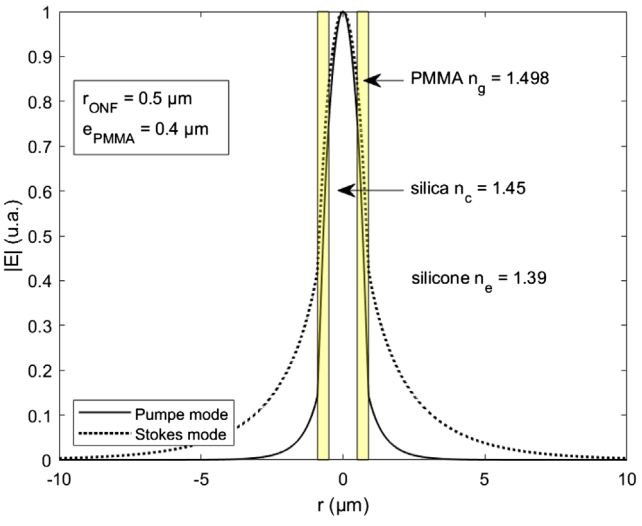

Figure 3. Profile of the pump and Stokes modes propagating in an ONF having a radius of 500 nm, coated by a 400 nm thick layer of PMMA and embedded in silicone.

of TiO_2 with thicknesses of between 20 and 80 nm. We observe an optimum radius around 250–300 nm, slightly depending on the thickness of the layer. Modal Raman gains above the targeted value of 0.2 m^{-1} W^{-1} can be largely achieved even for large radii, which will alleviate the constraints on the geometry of the ONF or the input pump power. As an example, with an ONF radius of 500 nm and a TiO_2 layer of 60 nm thick, a modal Raman gain of 0.44 m^{-1} W^{-1} is obtained. As a thumb rule, the product $\gamma = g_{\mathrm{Rmod}} \times L \times P_p$, where P_p is the input pump power, has to be equal to 20 to get the Stokes output power equal to the pump output power. This value can be obtained with an ONF of only 1 cm in length and a moderate peak input power of 350 W.

4 ONF coated with PMMA (ONF 2)

In this study, ONF coated with PMMA has been encapsulated with a low-index polymer of silicone ($n_{\mathrm{silicone}} = 1.39$). This material has the advantage of being polymerized in mass for mm deposition. This encapsulation enables to enhance the mechanical resistance of the ONF and to keep the guidance at the same time. The refractive index of PMMA is 1.49. In [10] its Raman gain coefficient has been measured at 631 nm. By taking into account its spectral dependency we found a value of 2.78 × 10^{-12} mW^{-1} at 1.5 µm. The pump wavelength is 1.06 µm. The Raman shift of PMMA being 2957 cm^{-1}, the first Stokes order wavelength is at 1.53 µm.

Figure 3 shows an example of calculated spatial modes at the pump and Stokes wavelengths for an ONF radius of 0.5 µm, a PMMA layer of 400 nm thick, encapsulated in silicone. In this configuration, due to the large difference between the pump and Stokes modes wavelengths, the spatial overlap between the two waves is not as strong as for ONF 1, which will induce a lower modal Raman gain.

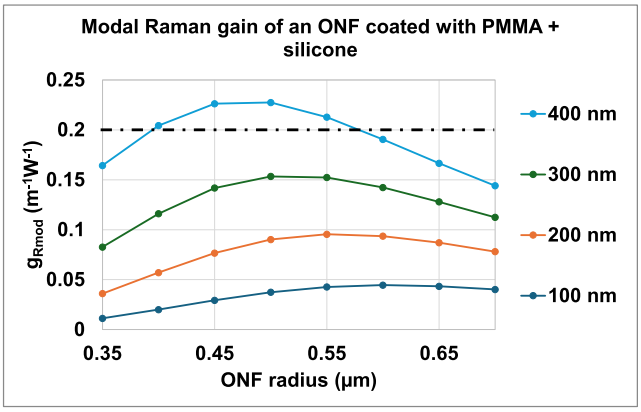

Figure 4. Modal Raman gain versus the ONF radius in function of the thickness of the PMMA layer.

Figure 4 shows the modal Raman gain of ONF 2 *versus* the ONF radius for deposited layers of PMMA with thicknesses of between 100 and 400 nm. The optimum radius is around 0.5 µm, depending on the thickness of the PMMA layer. Modal Raman gains above 0.2 m^{-1} W^{-1} can be achieved but PMMA thickness should be around 400 nm, which will need multiple layers of deposition [11]. As an example, with an ONF radius of 500 nm and a PMMA layer of 400 nm thick, a modal Raman gain of 0.22 m^{-1} W^{-1} is obtained. $\gamma \simeq 20$ for an ONF length L of 1 cm and a peak input power of 1 kW. At first sight, ONF 2 seems less promising than ONF 1, due to a Raman coefficient which is almost three times lower than the one of TiO_2. However, as the laser damage threshold of PMMA is high, we believe this solution remains interesting since the lower Raman gain could be compensated by an increase of the pump power. Moreover, PMMA can be doped with dyes such as DR1 which can extend the range of applications [14].

5 Conclusion and perspectives

In this work, we have presented the design of new Raman wavelength converters based on ONF coated with two nonlinear materials, TiO_2 and PMMA. Our simulations show that SRS can be obtained with moderate input peak powers and typical ONF geometrical parameters (radius and length) and TiO_2 layer thicknesses. Even though the Raman gain is lower and the technical realization is more challenging, the solution with the PMMA coating should be considered. Moreover, we have shown in previous studies on laser-induced damage threshold in ONF that a bare ONF with a radius of 0.45 µm can already sustain peak powers above 700 W [8]. The same ONF immersed in a liquid, and hence protected, was able to sustain more peak power than available, *i.e.* more than 1 kW. As this threshold increases with the radius, we believe we will be able to push up the input power in the designed coated ONF without generating optical damages to increase the generated Stokes power.

These composite ONFs open the way to new experiments in nonlinear optics for the realization of all-fibered functions [15]. For example, the coating can enable to tailoring of the chromatic dispersion for the control of phase-matching conditions. The use of other nonlinear materials such as doped polymers opens new applications in the field of nonlinear optics and lasers.

Funding

The work was supported by the French National Research Agency (FUNFILM-ANR-16-CE24-0010-03).

Conflicts of interest

The authors declare that there are no conflicts of interest related to this article.

Data availability statement

This article has no associated data generated.

Author contribution statement

Sylvie Lebrun supervised the project, wrote the article and made the calculations for the design of the Raman converters. Maha Bouhadida and Abderrahim Azzoune contributed to the theoretical simulations. Laurent Divay supervised the choice of the chosen materials for the coatings. Théo Dampt and Mathieu Fauvel contributed to the determination of the parameters of the coatings. Christian Larat and Jean-Charles Beugnot participated in all the discussions related to this work and reviewed the manuscript.

References

1 Tong LM et al., Subwavelength-diameter silica wires for low-loss optical wave guiding, *Nature* **426**, 816–819 (2003).
2 Corzo N et al., Waveguide-coupled single collective excitation of atomic arrays, *Nature* **566**, 359 (2019).
3 Delaye P et al., Gas-pressure tuning of wavelength of photon pair emitted by Four-Wave-Mixing in Nanofibers, *PRA* **104**, 063715 (2021).
4 Zhang L et al., Micro-/nanofiber optics: merging photonics and material science on nanoscale for advanced sensing technology, *Science* **23** (1), 100810 (2020).
5 Haddad Y et al., Microscopic imaging along tapered optical fibers by right-angle Rayleigh light scattering in linear and nonlinear regime, *Opt. Express* **29** (24), 39159–39172 (2021).
6 Bouhadida M et al., Highly efficient and reproducible evanescent Raman converters based on a silica nanofiber immersed in a liquid, *Appl. Phys. B* **125**, 228 (2019).
7 Fanjoux G et al., Demonstration of the evanescent Kerr effect in optical nanofibers, *Opt. Express* **27**, 29460–29470 (2019).
8 Bouhadida M et al., Operating range of efficient Raman converters based on nanofibers immersed in different liquids, *IEEE Photonics Technol. Lett.* **33** (17), 967–970 2021.
9 Evans C et al., Spectral broadening in anatase titanium dioxide waveguides at telecommunication and near-visible wavelengths, *Opt. Express* **21**(15), 18582 (2013).

10 Thomas KJet al., Raman spectra of polymethyl methacrylate optical fibres excited by a 532 nm diode pumped solid state laser, *J. Opt. A Pure Appl. Opt.* **10**, 055303 (2008).
11 Divay L et al., *IEEE Phot. Techn. Lett.* (to be published).
12 Snyder AW et al., *Optical waveguide theory* (Springer Science & Business Media, London, New York, 2012).
13 Turner MD et al., A full vectorial model for pulse propagation in emerging waveguides with subwavelength structures part II: stimulated Raman Scattering, *Opt. Express* **17**(14), 11565–11581, (2009).
14 Sugita A et al,, Second-Order Nonlinear Optical Susceptibilities of Nonelectrically Poled DR1–PMMA Guest–Host Polymers*J. Phys. Chem. B* **117** (47)14857–14864, (2013).
15 Azzoune A et al., Modeling photon pair generation by second-order surface nonlinearity in silica nanofibers, *J. Opt. Soc. Am. B* **38**, 1057–1068 (2021).